

# Novel low-cost hybrid composites from asphaltene/SBS tri-block copolymer with improved thermal and mechanical properties

Hongchao Wu<sup>1</sup> · Vijay Kumar Thakur<sup>3</sup> · Michael R. Kessler<sup>1,2,3</sup>

Received: 17 August 2015 / Accepted: 29 October 2015 / Published online: 12 November 2015  
© Springer Science+Business Media New York 2015

**Abstract** A continuous demanding in raw chemicals cost reduction and processing simplification facilitates the exploration and development of new materials in current plastics industries. In this study, a novel carbonaceous filler material “asphaltene” extracted from inexpensive and abundant asphalt is blended into a thermoplastic elastomer poly(styrene–butadiene–styrene) copolymer (SBS) for the fabrication of hybrid composites at different loadings via melt-compounding. Due to its intrinsic molecular rigidity and desirable compatibility with SBS, the prepared asphaltene/SBS composites displays excellent thermo-mechanical properties by improving the storage modulus in the glassy region by 19 % and in the rubbery region by 305 %, as well as increasing the thermal stability by up to 20 °C. The overall mechanical properties are also enhanced substantially by incorporation of asphaltene into the SBS matrix according to the filler loading in SBS: the tensile strength increased by 2.2 MPa, the maximum elongation by 268 %, Young’s modulus by 214 %, and toughness by 100.4 %. Although the introduced asphaltene inevitably led to a gradual increment in the viscosity of polymer melts from the filler–filler and filler–polymer interactions, homogeneous dispersion of the reinforcing fillers at optimum loading (20–30 wt%) in SBS matrix is still sustained.

## Introduction

Poly(styrene–butadiene–styrene) tri-block copolymer (SBS) is one of the most important commercially available thermoplastic elastomers (TPEs) that consists of two distinct phases morphology: the glassy polystyrene (PS) domains have been found to be covalently connected with rubbery polybutadiene (PB) segments [1, 2]. By owning mechanical properties such as softness, flexibility, and extensibility that similar to most of other synthetic and natural rubber [3], SBS exhibits several other advantages such as damping properties, chemical resistance, and electrical insulation as well [4]. In order to modify the thermal, mechanical, and electrical properties, SBS is not only investigated by incorporation with various inexpensive fillers such as carbon black [5], carbon nanotubes [6–9], carbon fiber [10], clay [11–13], and soy flour [14], but also extensively explored for the preparation of polymer blends with poly(2,6-dimethyl-1,4-phenylene oxide) [15], polyaniline [16–18], and thermoplastic polyurethane [3].

In the field of road construction, a great amount of works were investigated by applying SBS as modifier to improve the performance and durability of bitumen. Although the SBS-modified asphalt displays encouraging improvement in some properties including viscoelastic [19, 20] and dynamic mechanical performance [21], elastic recovery [22], stiffness modulus [23], and rutting resistance [24], the storage stability of SBS-modified asphalt at elevated temperatures is negatively impacted due to the mismatch in the density, polarity, and molecular weight of the two immiscible phases [25]. In order to overcome this issue by improving the compatibility between SBS and asphalt, various strategies were performed including end-groups functionalization [26], monomer grafting [27, 28], sulfur vulcanization [2, 29, 30], and hydrophobic clay minerals compounding [31, 32].

✉ Michael R. Kessler  
MichaelR.Kessler@wsu.edu

<sup>1</sup> Department of Materials Science and Engineering, Iowa State University, Ames, IA, USA

<sup>2</sup> Ames Laboratory, US Department of Energy, Ames, IA, USA

<sup>3</sup> School of Mechanical and Materials Engineering, Washington State University, Pullman, WA, USA

Asphaltene is known as the heaviest hydrocarbons component in the asphalt along with paraffins, resins, aromatics, and naphthenes [33]. The chemical characteristics and molecular mass of asphaltene is difficult to determine accurately due to its structural complexity that is associated with the crude oil source and the strong propensity of self-aggregation. However, it is well acknowledged that the general molecular structure of asphaltene contains alicyclic and side aliphatic chains that surround on a poly-condensed aromatic and naphthenic units core substituted with minority of heteroatoms such as nitrogen, sulfur, and oxygen, and traces of metal elements [34]. On the other hand, inter- and intra-molecular interactions including hydrogen bond,  $\pi$ - $\pi^*$  stacking force [35, 36], polarity induction forces [37], and electrostatic attractions [38, 39] are correlated to the flocculation and self-aggregation of asphaltene by forming the colloidal particles as the coke-like precursor, which is responsible for the blockage of transfer pipelines [40] and the deactivation of catalytic reaction in the oil upgrading and refining processes [41].

Although many research efforts have been made to perform the structure analysis of extracted asphaltene from different crude oils [42, 43] and treated with various processes towards asphaltene [34, 44], scarce attention has been focused on its potential application other than the source of pure carbon microsphere [45] and carbon fibers [46]. Recently, we reported a study to evaluate the reinforcing effect of asphaltene as novel low-cost filler in epoxy resin after the molecular modification with silane coupling agents [47]. However, the overall reinforcement seemed to be constrained by the maximum of filler loading (5 wt%) due to the processing difficulty associated with the high viscosity of thermoset suspensions. For further investigation of its reinforcing effect in polymer matrix, the extracted asphaltene will be blended into SBS copolymer at very high loading (up to 50 wt%) via melt-compounding method for fabrication of the low-cost and high-performance hybrid TPEs in the fields of automotive industries (pneumatic tire), household appliance (footwear), construction, and building materials (adhesives and sealants).

## Experimental

### Materials

The source of asphaltene, asphalt (Asphalt-All Grade), was obtained from the Road Science, LLC (Tulsa, Oklahoma). The *n*-heptane (HPLC) and toluene (Reagent) were all obtained from Fisher Scientific and were used directly without further purification in this experiment. The

poly(styrene-butadiene-styrene) rubber was purchased from Polyone Distribution (Romeoville, Illinois).

### Extraction of asphaltene

The asphaltene was extracted from the asphalt through SARA (saturates-aromatics-resins-asphaltenes) fractionation strategy followed by the previously studies [34, 47]. Specifically, the asphalt was firstly dissolved in toluene with mass/volume ratio of 1:5 and mixed for 1 h at 60 °C. The mixture was then filtered with 0.45- $\mu$ m filter membrane to separate the filtrate and undissolved components. After the removal of toluene with a rotary vaporator, the toluene-free asphalt was further mixed with *n*-heptane at a mass/volume ratio of 1:40 for another 4 h at 80 °C. Following that, the mixture was left in a dark cabinet overnight for fully precipitation. Afterward, the mixture was filtered with 0.45- $\mu$ m filter membrane to collect the non-filterable substance (asphaltene). To remove the residual waxy substance, asphaltene was further purified by merging in boiled *n*-heptane in a Soxhlet apparatus for at least 24 h until the filtrate solution became colorless. Ultimately, the obtained dark-brown solid asphaltene was dried in a vacuum oven at 70 °C overnight to evaporate the *n*-heptane and was referred as the final product to be used as filler material after gently grinded into fine powders. The chemical analysis and molecular characterization of asphaltene is given in details from our recent work [47], revealing that the as-prepared asphaltene contains 84 % of C and 7 % heteroatomic elements (N, S, and O), which intersperse in the molecular structure composing of 6–7 fused aromatic rings, along with the aggregation morphology as micro-sized plate-like particles.

### Preparation of asphaltene/SBS hybrid composites

The SBS and asphaltene were physically blended with different compositions at a mixing speed of 65 rpm in a twin-screw microcompounder (DACA Instrument, Santa Barbara, CA) at 180 °C for 15 min to facilitate homogeneous melt-compounding. Subsequently, the extruded samples were compressed into square plates (dimension of 50 × 50 × 1 mm) on a compression molding machine (Wabash MPI, IN, USA) at 180 °C under a pressure of 1500 psi for 30 min. After temperature cool down and pressure relief, the obtained samples were cut into specific shapes for different measurements: circular specimens with a diameter of 25 mm were prepared for rheology measurement; five pieces of 15 × 5 × 1 mm rectangular specimens from each composition were used for dynamic mechanical analysis; and three pieces standard dog-bone specimens were made for tensile test.

## Characterization of asphaltene/SBS hybrid composites

The rheological properties of composites were performed on an AR2000EX rheometer (TA Instruments) under oscillatory shear measurement in frequency sweep testing mode at 180 °C. A Q50 thermogravimetric analyzer (TGA) from TA Instruments was employed to study the thermal stability of asphaltene/SBS hybrids under nitrogen atmosphere. Dynamic mechanical properties of specimen were measured from −100 to 120 °C at 3 °C/min on a Q800 dynamic mechanical analyzer (DMA) from TA Instruments using tension clamp in constant strain (0.05 %) mode. The tensile test was performed on Instron at extension rate of 50.0 mm/min using a static load cell ( $\pm 2$  kN) at room temperature. The fresh fracture surfaces of asphaltene/SBS composites after the tensile test were characterized with a FEI Quanta 250 field emission scanning electron microscope (FE-SEM) at 10.00 kV under high vacuum. The particle size was estimated by image analysis software ImageJ.

## Results and discussion

### Rheological analysis

Rheological behavior is an imperative parameter to optimize the processing condition for thermoplastics extrusion. Figure 1 plots the dynamic frequency dependence of the absolute value of complex viscosities ( $|\eta^*|$ ) and shear modulus ( $G'$ ) among neat SBS and asphaltene/SBS composites at the same temperature during the melt-compounding process (180 °C). According to an order–disorder transition (ODT) theory in the majority of block copolymers, which demonstrates the disappearance of ordered

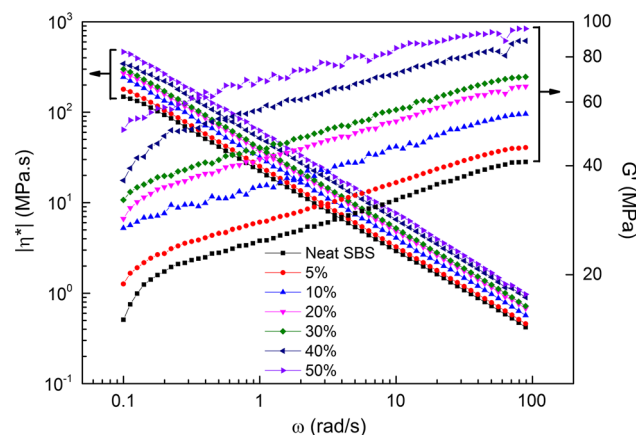


**Fig. 1** Comparison of  $|\eta^*|$  and  $G'$  of asphaltene/SBS composites at 180 °C

micro-domain (formed by phase-separation of PS and PB) and the formation of disordered mono-phase fluid as the temperature exceeds a critical value [48, 49], both the pure SBS and its composites melts showed a Newtonian and shear-thinning behavior over oscillation frequencies ( $\omega$ ) ranging from 0.1 to 100 rad/s. Since the  $|\eta^*|$  reflects the viscoelastic property of polymeric materials, a gradual increase in the  $|\eta^*|$  of SBS by the involvement of asphaltene could be interpreted from the filler–filler and the filler–matrix interactions: one the one hand, mutual attraction force such as  $\pi$ – $\pi^*$  stacking and van der Waal's might result in the formation of inter-aggregation [50] among asphaltene particles based on its aromaticity and polarity; on the other hand, the introduced asphaltene particles tend to physically hinder and anchor the free movement of PB segments in the fully segregated and heterogeneous multi-phase system at 180 °C [51], as illustrated in Fig. 2. Furthermore,  $G'$  of the hybrid composites also exhibited a gradual increment as the filler loading increased in the SBS, which was mainly attributed to the stiffness imparted to the overall matrix by the rigid asphaltene particles. Reversely, the addition of SBS into asphalt also modified the rheological performance of base bitumen by increasing the complex modulus [20] and viscosity [19].

### Thermogravimetric analysis

Thermal degradation behaviors of pristine asphaltene, neat SBS, and asphaltene/SBS composites were investigated in inert nitrogen atmosphere. Figure 3a shows that approx. 55 wt% residual char was left after pyrolysis of asphaltene. The carbonaceous material experienced a significant weight loss between 350 and 550 °C, with the major weight loss peak at approx. 470 °C as referred from the derivative weight changes curve in Fig. 3b, which corresponded to the collapse of asphaltene's molecular structure [52]. Above 600 °C, no further weight loss was detected during pyrolysis. On the other hand, the SBS copolymer thermally degraded between 250 and 470 °C, exhibiting two major weight loss peaks at approx. 340 and 450 °C, which were attributed to the decomposition and volatilization of the polymeric components [53, 54]. As asphaltene incorporated into the matrix, the weight loss curve of the composites presented an additional shoulder about 450 °C, which could be associated with the decomposition of asphaltene in the SBS. Moreover, the actual fraction of fillers blended in the melt-compounding at different loading levels could be estimated from the residual weight percent of composites after the pyrolysis, as presented in the inset of Fig. 3a. Table 1 includes the thermal degradation temperatures at 5 and 10 wt% weight loss of each specimen. The higher thermal stability of asphaltene facilitated an enhancement of SBS's thermal

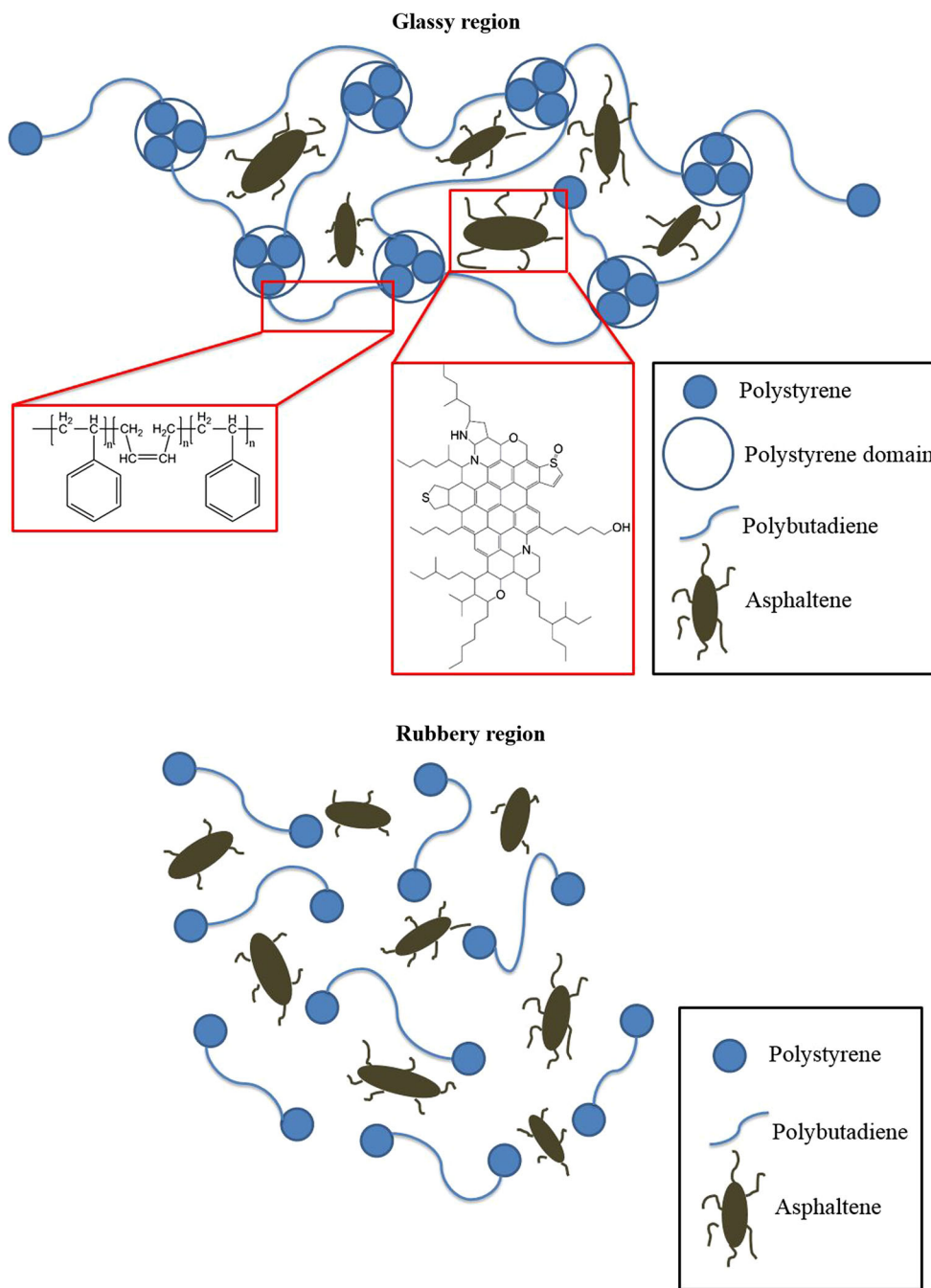


**Fig. 2** Schematic illustration of heterogeneous phases in asphaltene/SBS composites

decomposition temperature, guaranteed the potential high-temperature application of this new composite material.

**Dynamic mechanical analysis**

Figure 4a depicts the dynamic mechanical properties of asphaltene/SBS composites over the measured temperature between  $-100$  and  $120$  °C. First of all, at any given loading, elastic modulus ( $E'$ ) did not show a significant

enhancement in the glassy region, whereas a noticeable increment was found in its rubbery region, especially as the filler loading was above 30 wt%. In addition, the suppression of  $\tan \delta$  peak height manifests the intercalated asphaltene constrained the dynamic mobility of PB segments during the glassy-rubbery transition. By considering the glass transition temperatures ( $T_g$ ) of pure PB ( $\approx -100$  °C) and PS ( $\approx 100$  °C), due to the microphase separation from the partial miscibility among the two

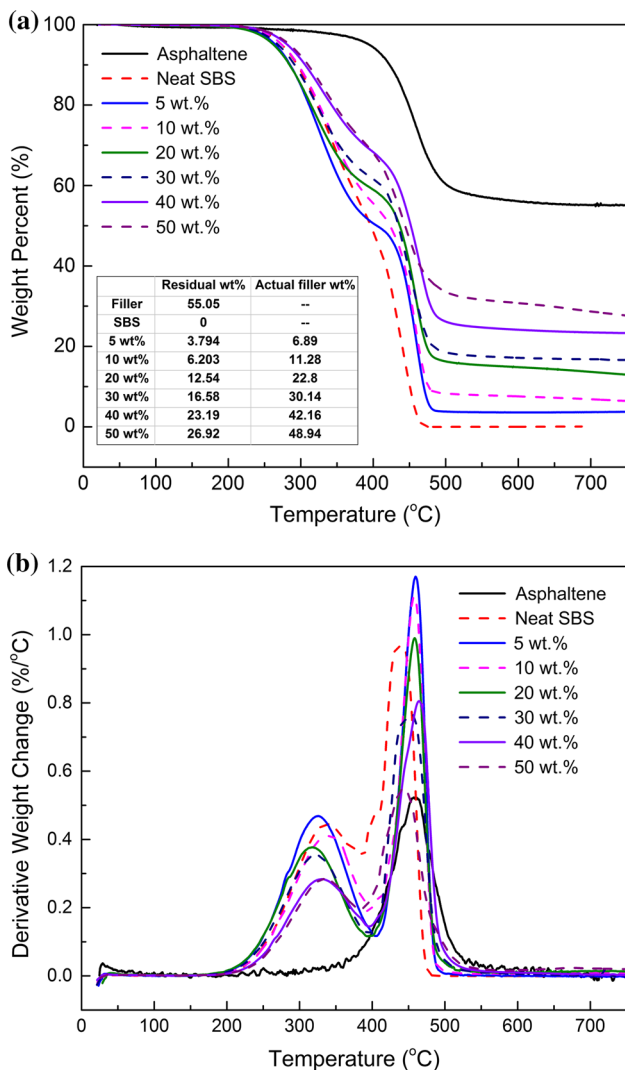


**Fig. 3** Comparison of **a** thermal degradation and **b** derivative weight changes of the asphaltene/SBS composites under nitrogen atmosphere

segments and a relatively low concentration of PS phase, the  $T_g$  of PB segment shifted to higher temperature ( $\approx -39^\circ\text{C}$ ) along with the absence of  $T_g$  of PS [14]. In comparison with neat SBS,  $T_g$  was slightly impacted by the presence of asphaltene, at high loading levels (40 and 50 wt%). Similar to carbon black [50], the interaction between asphaltene and SBS is primarily based on the physisorption effect: polybutadiene phases became less flexible as a higher amount of asphaltene dispersing in the matrix [55]. Figure 4b provides a quantitative analysis regarding the influence of fillers on  $E'$  in glassy ( $-100^\circ\text{C}$ ) and rubbery ( $25^\circ\text{C}$ ) regions of the hybrid materials. Although  $E'$  gradually improved in both regions upon the filler loading, a more pronounced strengthening effect was recognized at the rubbery region. Specifically at 50 wt% loading, in comparison with the increment extent in glassy region (19 %),  $E'$  skyrocketed by 305 % in rubbery region.

**Table 1** Thermal stability of asphaltene and asphaltene/SBS composites under nitrogen atmosphere. The error bars represent the standard deviation based on four specimen

	Neat SBS	5 wt%	10 wt%	20 wt%	30 wt%	40 wt%	50 wt%
Filler							
Temperature at 5 % weight loss ( $^\circ\text{C}$ )	$394.39 \pm 10.98$	$265.94 \pm 6.56$	$269.56 \pm 5.51$	$272.01 \pm 5.87$	$274.47 \pm 5.09$	$277.16 \pm 3.36$	$279.75 \pm 3.88$
Temperature at 10 % weight loss ( $^\circ\text{C}$ )	$428.20 \pm 4.92$	$282.62 \pm 3.98$	$291.44 \pm 5.85$	$296.02 \pm 9.11$	$297.34 \pm 5.6$	$301.52 \pm 3.62$	$303.04 \pm 5.94$

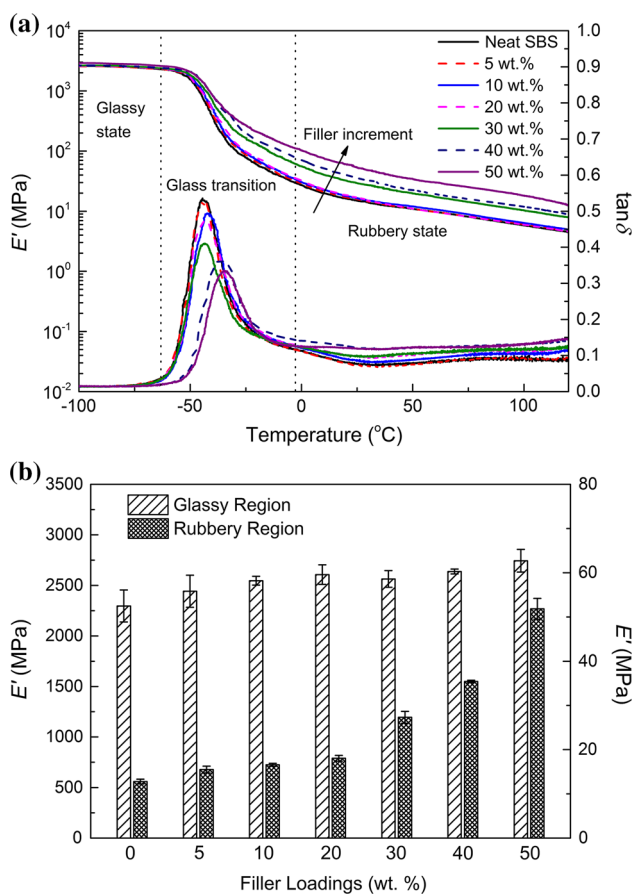


**Fig. 4** Comparison of asphaltene/SBS composites: **a** dynamic mechanical behaviors; **b**  $E'$  at glassy and rubbery regions. The error bars represent standard deviations based on five samples

According to Fig. 2, formation of PS domain from the physical aggregation among PS blocks contributes to the intermolecular crosslinked network and offers the rigidity of SBS in glassy region, which might overshadow the stiffness of asphaltene in this ordered molecular structure; whereas such crosslinked network disappears due to the dissociation of PS domains at higher temperature [56], and then the strengthening behavior of asphaltene becomes more pronounced in the disordered and segregated rubbery region. A similar reinforcing effect in SBS system was also reported by blending in polyaniline [16] and carbon black [5], respectively.

**Mechanical property and fracture surfaces analysis**

In this work, tensile test was performed to study the mechanical properties of asphaltene/SBS composites. Figure 5 indicates that neat SBS tri-block copolymer exhibited a rubber-like plastic deformation and significant elongation

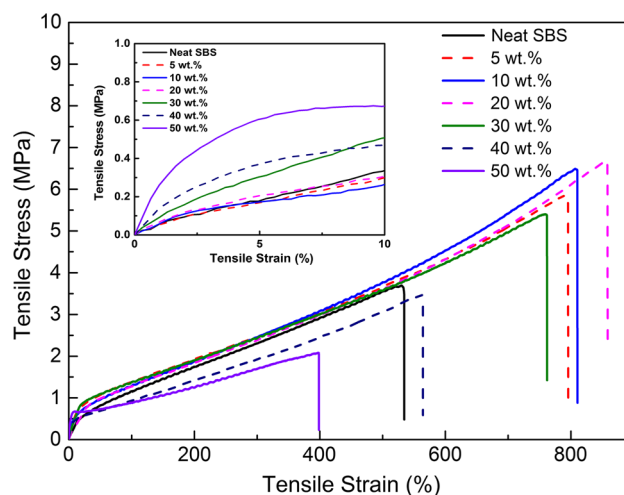


**Fig. 5** Comparison of stress–strain curves of asphaltene/SBS composites

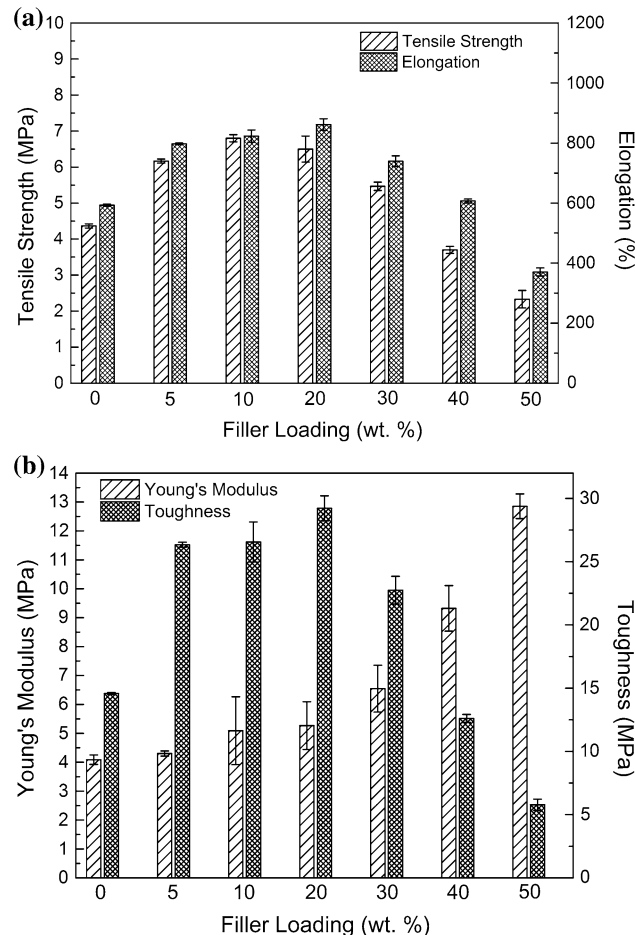


**Fig. 6** Comparison of **a** tensile strength and elongation at break; **b** Young’s modulus and toughness for asphaltene/SBS composites. The error bars represent standard deviations based on three samples

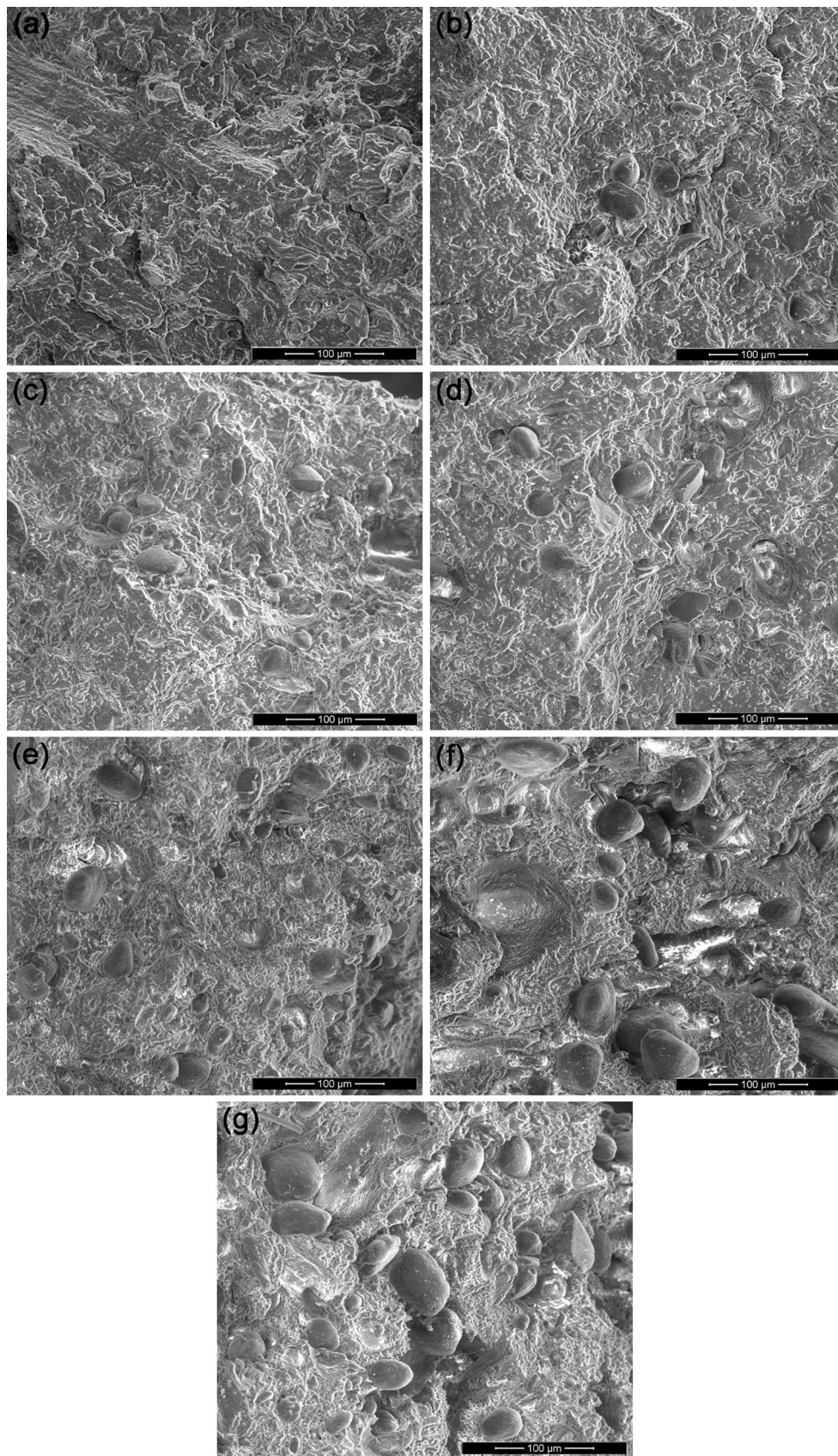


**Fig. 7** SEM images of fracture surface of asphaltene/SBS composites: **a** neat SBS; **b** 5 wt%; **c** 10 wt%; **d** 20 wt%; **e** 30 wt%; **f** 40 wt%; **g** 50 wt%

behavior prior to fracture. Besides that, given the reinforcement of PS segments in PB domain, only one yield point was shown in the first elongation region followed by a continuous increment in tensile stress according to the stress–strain ( $\sigma$ – $\epsilon$ ) curve of SBS copolymer, which was different from the most natural or synthetic crosslinked rubbers by showing “S-shaped”  $\sigma$ – $\epsilon$  curve. In comparison of neat SBS, the  $\sigma$ – $\epsilon$  curves of hybrid materials containing asphaltene displayed the similar behaviors. However, it is interesting to observe that tensile strength and elongation were dependent on the weight percent of asphaltene in SBS: both properties increased initially from 5 to 20 wt% and then decreased systematically from 30 to 50 wt%. Furthermore, as demonstrated in the inset of Fig. 5, the slopes of  $\sigma$ – $\epsilon$  curve increased within 5 % tensile strain, indicating a steady enhancement in Young’s modulus among asphaltene/SBS composites upon the filler loading.

Figure 6a demonstrates the tensile strength and elongation at break for the prepared specimen. Neat SBS showed the identical mechanical properties as the previous study [14], demonstrating an excellent reproducibility of the product. In terms of asphaltene/SBS composites, both tensile strength and elongation increased by 2.2 MPa and by 268 % from 0 to 20 wt%, respectively. The improvement of mechanical properties might be originated from the promising compatibility between filler and matrix by the presence of  $\pi$ – $\pi^*$  physical stacking force as the composites prepared from melt-compounding [6], and meanwhile, the intrinsic rigid molecular structure of asphaltene further imparted the reinforcing effect toward SBS matrix. However at higher loadings, the deterioration of mechanical properties could be due to the agglomeration of asphaltene particles, which gave rise to the non-uniform distribution of stresses under tension stress. Such assumption will be confirmed from the fracture topography of specimens as discussed in the following section. Young’s modulus, on the other hand, reflecting the stiffness of a material, is primarily dependent on the elastic filler contents in polymer composites [57]. Figure 6b depicts a substantial and gradual increase in the Young’s modulus (determined from 0.5–2.5 % elongation) by the presence of higher loading of stiff asphaltene filler in the SBS matrix. In particular,  $E_{0.5-2.5\%}$  increased from 4.1 MPa for neat SBS to 12.8 MPa (by 214 %) as 50 wt% asphaltene particles incorporated into the copolymer, as in good agreement with the constant improvement of elastic modulus from rheological and dynamic mechanical measurement. However, the toughness calculated from the area of  $\sigma$ – $\epsilon$  curve followed the similar trend of tensile stress and strain upon the filler increment.

The fracture surface of SBS and its composites were characterized with SEM after the tensile test. In comparison of neat SBS, the fracture surfaces of composites were

similar among all the samples at any given loading, demonstrating that asphaltene did not affect the ductile failure mechanism of SBS copolymer. As shown in Fig. 7, asphaltene had the tendency to agglomerate into ca. 30–50- $\mu$ m individual pebble-like particles during melt-compounding. Figure 7b, c, d, e displays the uniform dispersion of filler particles in the matrix at lower loadings; nonetheless, the inhomogeneous dispersion of particles was observed as the filler loading went up to 40 and 50 wt%, which could be one of the reasons attributing to the deterioration of the mechanical properties as suggested in the earlier section. Another plausible reason is associated with the agglomeration of particles at high weight percent, which served as stress concentrator that initiated cracks formation and facilitated their propagation the under external tensile force. Specifically, as Fig. 8 provides a quantification analysis of particle size distribution of asphaltene fillers in SBS at various loading levels, it could be noticed that the particle size distribution gradually shifted from 20–50  $\mu$ m to 40–80  $\mu$ m range or even larger when the intercalated fillers exceeded a critical loading at 30 wt%. Although Young’s modulus was not negatively affected, tensile strength and elongation suffered from degradation when the incorporated particles agglomerate

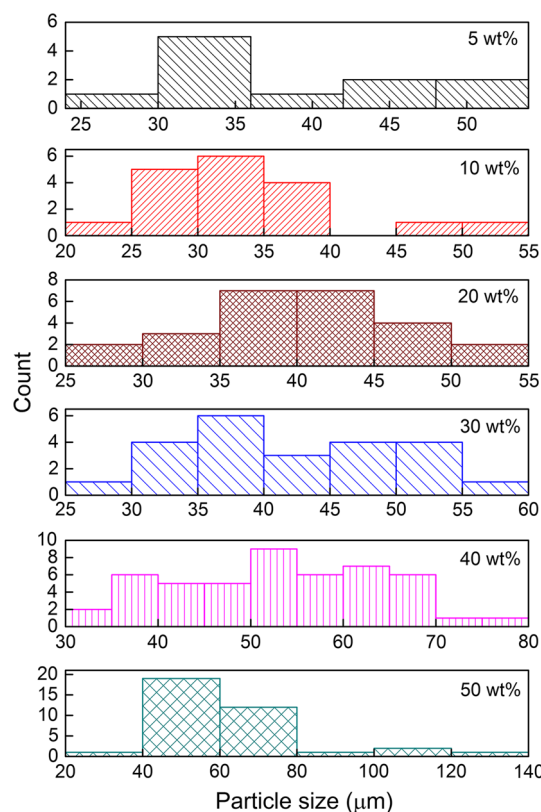


Fig. 8 Particle size distribution of asphaltene in SBS matrix at different filler loadings counted from different SEM fracture surfaces



into larger size at high filler loading [58]. As a result, the ideal portion of asphaltene in SBS (20–30 wt%) offered the most promising mechanical performance.

## Conclusion

The asphaltene extracted from raw asphalt was studied for novel application as low-cost filler in SBS composites from a melt-compounding process. According to the rheological measurement, both complex viscosity and shear storage modulus of SBS copolymer exhibited an increment upon blending with increasing loadings of asphaltene powders. Besides the improvement of thermal stability as the elevation of the decomposition temperature by 20 °C in the asphaltene/SBS hybrid materials, the incorporated fillers were also recognized for its reinforcement effect in glassy and especially in rubbery region by displaying a 305 % enhancement in storage modulus. Regarding the mechanical properties, the introduced asphaltene particles not only gradually improved the Young's modulus, but also enhanced the tensile strength, strain, and toughness of SBS matrix at lower filler concentration. In summary, the attractive inexpensive raw chemical, the desirable simple processing approach, the satisfying thermo-mechanical, and the excellent mechanical properties guarantee asphaltene/SBS hybrid material as a promising high-performance composites in TPE industries.

**Acknowledgements** The authors acknowledge funding for this project from Honeywell Federal Manufacturing & Technologies, LLC.

## References

1. Scott DB, Waddon AJ, Lin YG, Karasz FE, Winter HH (1992) Shear-induced orientation transitions in triblock copolymer styrene-butadiene-styrene with cylindrical domain morphology. *Macromolecules* 25:4175. doi:10.1021/ma00042a019
2. Wen G, Zhang Y, Zhang YX, Sun K, Fan YZ (2002) Rheological characterization of storage-stable SBS-modified asphalts. *Polym Test* 21:295. doi:10.1016/s0142-9418(01)00086-1
3. Wu JH, Li CH, Wu YT, Leu MT, Tsai Y (2010) Thermal resistance and dynamic damping properties of poly (styrene-butadiene-styrene)/thermoplastic polyurethane composites elastomer material. *Compos Sci Technol* 70:1258. doi:10.1016/j.compscitech.2010.03.014
4. Kricheldorf HR, Holden G, Quirk RP (2004) Thermoplastic elastomers. Hanser Publishers, Munich
5. Leyva ME, Barra GMO, Moreira ACF, Soares BG, Khastgir D (2003) Electric, dielectric, and dynamic mechanical behavior of carbon black/styrene-butadiene-styrene composites. *J Polym Sci Part B* 41:2983. doi:10.1002/polb.10627
6. Lu L, Zhou Z, Zhang Y, Wang SF, Zhang YX (2007) Reinforcement of styrene-butadiene-styrene tri-block copolymer by multi-walled carbon nanotubes via melt mixing. *Carbon* 45:2621. doi:10.1016/j.carbon.2007.08.025
7. Pedroni LG, Soto-Oviedo MA, Rosolen JM, Felisberti MI, Nogueira AF (2009) Conductivity and mechanical properties of composites based on MWCNTs and styrene-butadiene-styrene block (TM) copolymers. *J Appl Polym Sci* 112:3241. doi:10.1002/app.29897
8. Pedroni LG, Araujo JR, Felisberti MI, Nogueira AF (2012) Nanocomposites based on MWCNT and styrene-butadiene-styrene block copolymers: effect of the preparation method on dispersion and polymer-filler interactions. *Compos Sci Technol* 72:1487. doi:10.1016/j.compscitech.2012.06.009
9. Costa P, Silva J, Sencadas V, Simoes R, Viana JC, Lanceros-Mendez S (2013) Mechanical, electrical and electro-mechanical properties of thermoplastic elastomer styrene-butadiene-styrene/multiwall carbon nanotubes composites. *J Mater Sci* 48:1172. doi:10.1007/s10853-012-6855-7
10. Ibarra L, Panos D (1997) Mechanical properties of thermoplastic butadiene-styrene (SBS) and oxidized short carbon fibre composites. *Polym Int* 43:251
11. Zhang W, Zeng J, Liu L, Fang Y (2004) A novel property of styrene-butadiene-styrene/clay nanocomposites: radiation resistance. *J Mater Chem* 14:209. doi:10.1039/b307978c
12. Zhang ZJ, Zhang LN, Li Y, Xu HD (2006) Styrene-butadiene-styrene/montmorillonite nanocomposites synthesized by anionic polymerization. *J Appl Polym Sci* 99:2273. doi:10.1002/app.22768
13. Wang ZB, Wang X (2011) Preparation and mechanical properties of styrene-butadiene-styrene tri-block copolymer/partly exfoliated montmorillonite nanocomposites prepared by melt-compounding. *J Thermoplast Compos Mater* 24:83. doi:10.1177/0892705710376471
14. Thakur VK, Grewell D, Thunga M, Kessler MR (2014) Novel composites from eco-friendly soy flour/SBS triblock copolymer. *Macromol Mater Eng* 299:953. doi:10.1002/mame.201300368
15. Tucker PS, Barlow JW, Paul DR (1988) Thermal, mechanical, and morphological analyses of poly(2,6-dimethyl-1,4-phenylene oxide)/styrene-butadiene-styrene copolymer blends. *Macromolecules* 21:1678. doi:10.1021/ma00184a026
16. Leyva ME, Soares BG, Khastgir D (2002) Dynamic-mechanical and dielectric relaxations of SBS block copolymer: polyaniline blends prepared by mechanical mixing. *Polymer* 43:7505. doi:10.1016/s0032-3861(02)00613-4
17. Leyva ME, Barra GMO, Gorelova MM, Soares BG, Sens M (2001) Conducting SBS block copolymer-polyaniline blends prepared by mechanical mixing. *J Appl Polym Sci* 80:626. doi:10.1002/1097-4628(20010425)80:4<626::aid-app1138>3.0.co;2-7
18. Soares BG, Leyva ME (2007) Effect of blend preparation on electrical, dielectric, and dynamical-mechanical properties of conducting polymer blend: SBS triblock copolymer/polyaniline. *Macromol Mater Eng* 292:354. doi:10.1002/mame.200600405
19. Martinez-Estrada A, Chavez-Castellanos AE, Herrera-Alonso M, Herrera-Najera R (2010) Comparative study of the effect of sulfur on the morphology and rheological properties of SB- and SBS-modified asphalt. *J Appl Polym Sci* 115:3409. doi:10.1002/app.31407
20. Topal A, Yilmaz M, Kok BV, Kuloglu N, Sengoz B (2011) Evaluation of rheological and image properties of styrene-butadiene-styrene and ethylene-vinyl Acetate polymer modified bitumens. *J Appl Polym Sci* 122:3122. doi:10.1002/app.34282
21. Fawcett AH, McNally T (2001) Blends of bitumen with polymers having a styrene component. *Polym Eng Sci* 41:1251. doi:10.1002/pen.10826
22. Chen JS, Huang CC (2007) Fundamental characterization of SBS-modified asphalt mixed with sulfur. *J Appl Polym Sci* 103:2817. doi:10.1002/app.24621
23. Kok BV, Yilmaz M (2009) The effects of using lime and styrene-butadiene-styrene on moisture sensitivity resistance of hot mix asphalt. *Constr Build Mater* 23:1999. doi:10.1016/j.conbuildmat.2008.08.019

24. Tayfur S, Ozen H, Aksoy A (2007) Investigation of rutting performance of asphalt mixtures containing polymer modifiers. *Constr Build Mater* 21:328. doi:[10.1016/j.conbuildmat.2005.08.014](https://doi.org/10.1016/j.conbuildmat.2005.08.014)
25. Wang T, Yi T, Yuzhen Z (2010) The compatibility of SBS-modified asphalt. *Pet Sci Technol* 28:764. doi:[10.1080/10916460902937026](https://doi.org/10.1080/10916460902937026)
26. Wang Q, Liao MY, Wang YR, Ren Y (2007) Characterization of end-functionalized styrene-butadiene-styrene copolymers and their application in modified asphalt. *J Appl Polym Sci* 103:8. doi:[10.1002/app.23867](https://doi.org/10.1002/app.23867)
27. Fu HY, Xie LD, Dou DY, Li LF, Yu M, Yao SD (2007) Storage stability and compatibility of asphalt binder modified by SBS graft copolymer. *Constr Build Mater* 21:1528. doi:[10.1016/j.conbuildmat.2006.03.008](https://doi.org/10.1016/j.conbuildmat.2006.03.008)
28. Cong PL, Chen SF, Chen HX (2011) Preparation and properties of bitumen modified with the maleic anhydride grafted styrene-butadiene-styrene triblock copolymer. *Polym Eng Sci* 51:1273. doi:[10.1002/pen.21934](https://doi.org/10.1002/pen.21934)
29. Zhang F, Yu JY, Wu SP (2010) Effect of ageing on rheological properties of storage-stable SBS/sulfur-modified asphalts. *J Hazard Mater* 182:507. doi:[10.1016/j.jhazmat.2010.06.061](https://doi.org/10.1016/j.jhazmat.2010.06.061)
30. Sun DQ, Ye F, Shi FZ, Lu WM (2006) Storage stability of SBS-modified road asphalt: preparation, morphology, and rheological properties. *Pet Sci Technol* 24:1067. doi:[10.1081/ft-200048186](https://doi.org/10.1081/ft-200048186)
31. Ouyang C, Wang SF, Zhang Y, Zhang YX (2005) Preparation and properties of styrene-butadiene-styrene copolymer/kaolinite clay compound and asphalt modified with the compound. *Polym Degrad Stab* 87:309. doi:[10.1016/j.polymdegradstab.2004.08.014](https://doi.org/10.1016/j.polymdegradstab.2004.08.014)
32. Yu JY, Wang L, Zeng X, Wu SP, Li B (2007) Effect of montmorillonite on properties of styrene-butadiene-styrene copolymer modified bitumen. *Polym Eng Sci* 47:1289. doi:[10.1002/pen.20802](https://doi.org/10.1002/pen.20802)
33. Silva SL, Silva AMS, Ribeiro JC, Martins FG, Da Silva FA, Silva CM (2011) Chromatographic and spectroscopic analysis of heavy crude oil mixtures with emphasis in nuclear magnetic resonance spectroscopy: a review. *Anal Chim Acta* 707:18. doi:[10.1016/j.aca.2011.09.010](https://doi.org/10.1016/j.aca.2011.09.010)
34. Chiaberge S, Guglielmetti G, Montanari L et al (2009) Investigation of asphaltene chemical structural modification induced by thermal treatments. *Energy Fuels* 23:4486. doi:[10.1021/ef900206n](https://doi.org/10.1021/ef900206n)
35. Alboudwarej H, Jakher RK, Svrcek WY, Yarranton HW (2004) Spectrophotometric measurement of asphaltene concentration. *Pet Sci Technol* 22:647. doi:[10.1081/ft-120034206](https://doi.org/10.1081/ft-120034206)
36. Painter PC, Sobkowiak M, Youtcheff J (1987) FT-IR study of hydrogen bonding in coal. *Fuel* 66:973. doi:[10.1016/0016-2361\(87\)90338-3](https://doi.org/10.1016/0016-2361(87)90338-3)
37. Anisimov MA, Yudin IK, Nikitin V et al (1995) Asphaltene aggregation in hydrocarbon solutions studied by photon correlation spectroscopy. *J Phys Chem* 99:9576. doi:[10.1021/j100023a040](https://doi.org/10.1021/j100023a040)
38. Acevedo S, Mendez B, Rojas A, Layrisse I, Rivas H (1985) Asphaltenes and resins from the Orinoco basin. *Fuel* 64:1741. doi:[10.1016/0016-2361\(85\)90402-8](https://doi.org/10.1016/0016-2361(85)90402-8)
39. Wilt BK, Welch WT, Rankin JG (1998) Determination of asphaltenes in petroleum crude oils by Fourier transform infrared spectroscopy. *Energy Fuels* 12:1008. doi:[10.1021/ef980078p](https://doi.org/10.1021/ef980078p)
40. Gentzis T, Rahimi PM (2003) A microscopic approach to determine the origin and mechanism of coke formation in fractionation towers. *Fuel* 82:1531. doi:[10.1016/S0016-2361\(03\)00032-2](https://doi.org/10.1016/S0016-2361(03)00032-2)
41. Bartholdy J, Andersen SI (2000) Changes in asphaltene stability during hydrotreating. *Energy Fuels* 14:52. doi:[10.1021/ef990121o](https://doi.org/10.1021/ef990121o)
42. Bouhadda Y, Bormann D, Sheu E, Bendedouch D, Krallafa A, Daaou M (2007) Characterization of Algerian Hassi-Messaoud asphaltene structure using Raman spectrometry and X-ray diffraction. *Fuel* 86:1855. doi:[10.1016/j.fuel.2006.12.006](https://doi.org/10.1016/j.fuel.2006.12.006)
43. Daaou M, Bendedouch D, Bouhadda Y, Vernex-Loset L, Modaressi A, Rogalski M (2009) Explaining the flocculation of Hassi Messaoud asphaltenes in terms of structural characteristics of monomers and aggregates. *Energy Fuels* 23:5556. doi:[10.1021/ef900596y](https://doi.org/10.1021/ef900596y)
44. Douda J, Llanos ME, Alvarez R, Bolanos JN (2004) Structure of maya asphaltene-resin complexes through the analysis of soxhlet extracted fractions. *Energy Fuels* 18:736. doi:[10.1021/ef034057t](https://doi.org/10.1021/ef034057t)
45. Wang XM, Guo JJ, Yang XW, Xu BS (2009) Monodisperse carbon microspheres synthesized from asphaltene. *Mater Chem Phys* 113:821. doi:[10.1016/j.matchemphys.2008.08.053](https://doi.org/10.1016/j.matchemphys.2008.08.053)
46. Natarajan A, Mahavadi SC, Natarajan TS, Masliyah JH, Xu ZH (2011) Preparation of solid and hollow asphaltene fibers by single step electrospinning. *J Eng Fiber Fabr* 6:1
47. Wu HC, Kessler MR (2015) Asphaltene: structural characterization, molecular functionalization, and application as a low-cost filler in epoxy composites. *RSC Adv* 5:24264. doi:[10.1039/c5ra00509d](https://doi.org/10.1039/c5ra00509d)
48. Tong JD, Jérôme R (2000) Synthesis of poly(methyl methacrylate)-b-poly(n-butyl acrylate)-b-poly(methyl methacrylate) triblocks and their potential as thermoplastic elastomers. *Polymer* 41:2499. doi:[10.1016/S0032-3861\(99\)00412-7](https://doi.org/10.1016/S0032-3861(99)00412-7)
49. Nojima S, Roe RJ (1987) Effect of molecular weight of added polystyrene on the order-disorder transition of styrene-butadiene diblock copolymer. *Macromolecules* 20:1866. doi:[10.1021/ma00174a029](https://doi.org/10.1021/ma00174a029)
50. Fröhlich J, Niedermeier W, Luginsland HD (2005) The effect of filler–filler and filler–elastomer interaction on rubber reinforcement. *Compos A* 36:449. doi:[10.1016/j.compositesa.2004.10.004](https://doi.org/10.1016/j.compositesa.2004.10.004)
51. Basseri G, Mazidi MM, Hosseini F, Aghjeh MKR (2014) Relationship among microstructure, linear viscoelastic behavior and mechanical properties of SBS triblock copolymer-compatible PP/SAN blend. *Polym Bull* 71:465. doi:[10.1007/s00289-013-1071-4](https://doi.org/10.1007/s00289-013-1071-4)
52. Murugan P, Mahinpey N, Mani T (2009) Thermal cracking and combustion kinetics of asphaltenes derived from Fosterston oil. *Fuel Process Technol* 90:1286. doi:[10.1016/j.fuproc.2009.06.008](https://doi.org/10.1016/j.fuproc.2009.06.008)
53. Su TT, Jiang H, Gong H (2009) Thermal stabilities and thermal degradation kinetics of a styrene-butadiene-styrene star block copolymer. *Polym Plast Technol Eng* 48:535. doi:[10.1080/03602550902824341](https://doi.org/10.1080/03602550902824341)
54. Lu L, Yu HY, Wang SF, Zhang Y (2009) Thermal degradation behavior of styrene-butadiene-styrene tri-block copolymer/multi-walled carbon nanotubes composites. *J Appl Polym Sci* 112:524. doi:[10.1002/app.29414](https://doi.org/10.1002/app.29414)
55. Fu BX, Lee A, Haddad TS (2004) Styrene-butadiene-styrene triblock copolymers modified with polyhedral oligomeric silsesquioxanes. *Macromolecules* 37:5211. doi:[10.1021/ma049753m](https://doi.org/10.1021/ma049753m)
56. Zhu J, Birgisson B, Kringos N (2014) Polymer modification of bitumen: advances and challenges. *Eur Polym J* 54:18. doi:[10.1016/j.eurpolymj.2014.02.005](https://doi.org/10.1016/j.eurpolymj.2014.02.005)
57. Fu SY, Feng XQ, Lauke B, Mai YW (2008) Effects of particle size, particle/matrix interface adhesion and particle loading on mechanical properties of particulate-polymer composites. *Compos Part B* 39:933. doi:[10.1016/j.compositesb.2008.01.002](https://doi.org/10.1016/j.compositesb.2008.01.002)
58. Zhu ZK, Yang Y, Yin J, Qi ZN (1999) Preparation and properties of organosoluble polyimide/silica hybrid materials by sol-gel process. *J Appl Polym Sci* 73:2977. doi:[10.1002/\(sici\)1097-4628\(19990929\)73:14<2977:aid-app22>3.0.co;2-j](https://doi.org/10.1002/(sici)1097-4628(19990929)73:14<2977:aid-app22>3.0.co;2-j)